Coda Q for the Sri Lankan Precambrian crust

Prasanna Gamage[1], Dr. Srikanth Venkatesan[2]

1. Corresponding Author. PhD student, School of Engineering and Science, Victoria University, Australia.
    Email: janakaprasanna.wepitiyagamage@live.vu.edu.au

2. Senior Lecturer, School of Engineering and Science, Victoria University, Australia.
    Email: srikanth.venkatesan@vu.edu.au

Abstract

Attenuation characteristics of the bedrock beneath Sri Lanka have been investigated analysing local seismic data recorded at the country's broadband seismic network. Digital high-gain records of 13 small to micro earthquakes, magnitude varying from M_L 1.5 to 3.6 in local magnitude scale, were processed for estimating coda Q. The standard single scattering model, which demands the decay rate of backscattered coda waves found at the tail part of seismograms, was applied at eight deferent frequency pass bands from 1 to 19 Hz. A parametric study by varying coda time window as 40, 50, 60 and 70 s, was carried out to examine the significance of time dependent behaviour in coda Q, if any. A trend of increasing Q with the length of time window at low frequencies, and a minor reversing trend at high frequencies were noted. The average variation of Q for all time windows was in the form, $Q = (301 \pm 17)f^{(0.67 \pm 0.02)}$.

Keywords: Coda Q, Single backscattering method, Attenuation, Sri Lanka

1. INTRODUCTION

Attenuation characteristics of seismic waves during propagation are considered to be carefully identified for a hazard study in a given region. These region specific characteristics are mostly associated with the inherent geotectonic features of the region. Thus, studying attenuation characteristics of a particular region would also be helpful to explore the featuring tectonic structures of the region.

Seismic wave attenuation through the basement rock, in respect to the most dominating phases such as S and Lg, can generally be parameterized into three categories depending on the mode of attenuation and on the local characteristics of the uppermost crust; (1) Geometric spreading (2) Anelastic whole path attenuation (3) Upper crustal attenuation. The geometric spreading or damping is commonly referred as a frequency independent parameter, which accounts attenuation in terms of wave scattering (reflections and refractions) that happens during travel through the crustal waveguide. For instance, in the typical trilinear form, the rate of geometric damping of direct waves at near-source distances (hypocentral distances up to about 70 km) has been noted as R^{-1} (R is the hypocentral distance). Consequently, at medium (between 70 to 130 or 140 km) and at far-source distances (hypocentral distances greater than 130 or 140 km) the rate differs to R^0 (due to compensatory effect of postcritical reflections and refractions at Moho and Conrad discontinuities) and to $R^{-0.5}$ (due to multiple reflections and refractions of body waves dominating regional phases), respectively (Atkinson and Boore 1995, Lam et al 2000). In some cases, a rapid near-source geometric attenuation than above (Atkinson 2004) and even frequency dependent attenuation rates (Atkinson 2005) have also been indicated. The anelastic attenuation accounts for decay in wave amplitude by the energy dissipation that takes place along the whole travel path of propagation. This energy dissipation entails intrinsic attenuation which may include heating of the heterogeneous medium, rearrangement or dislocation of particles during vibration of the medium, etc., which are considered as permanent losses of energy. Studies have also claimed that the decay rate, which is parameterized by the wave transmission quality factor (Q), includes wave scattering effects as well depending on the heterogeneity of the medium (Wu and Aki 1988). Moreover, evidence is available for the time dependency of Q resulted as a mean of changing the effective sampled volume with the time (Gusev 1995, Pulli 1984). Whole path attenuation or seismic absorption depends on the wave frequency in a manner which high frequency waves diminish more rapidly than that do low frequency waves. Importantly, this attenuation would be dominant for far-field or distant earthquakes for which the amount of attenuation is largely governed by the quality of the travelled medium. If the quality of crust is high, the wave propagation is good and vice versa. The upper crustal attenuation is also similar to the anelastic attenuation in the context of mechanism involved, although the parameter has primarily been considered capturing effects at the uppermost crust, probably at upper 3-4 km, where younger Sedimentary formations are abundant. As a norm, attenuations at the uppermost crust are examined separately from other path modifications mainly due to having higher attenuation rates at the uppermost part in comparison to that in mid and in deeper parts. The above discussed types of wave attenuation are generally case sensitive, i.e., the dominance of a particular type would be controlled by several other factors like site-source distance, wave frequency, crustal properties, local site characteristics, etc.

Sri Lanka is located in northern Indian Ocean more than thousand kilometres away from major plate boundaries. The country's location is often considered as aseismic, though, in many cases, the surrounding oceanic crust especially towards south southeast directions has been identified to be subjected to active intraplate seismicity (Royer and Gordon 1997, Stein

and Okal 1978, Wiens et al 1986). As evidenced by historical reports Sri Lanka has not indicated major/frequent local seismic activities during past decades except a few including a devastating one at the capital city-Colombo, which was happened on 14th of April 1615 with an estimated magnitude of the order of 6.4 in Moment magnitude scale (M_w). The event has incurred damage of 200 houses and caused over 2000 casualties (Wimalaratne 1993). The apparent sparse seismicity in the local context seems concentrating at areas where active local lineaments and faults are being present. Gamage and Venkatesan (2012) have given efforts in identifying such active areas in the country, by correlating reported events with local seismo-tectonic structures such as mega lineaments and shear zones especially located at geological boundaries. However, attenuation characteristics of the underlying crust have not been explicitly parameterized owing to lack of recorded data available for local events. Absence of a reliable seismic network and scarcity of good quality records were main barriers to be overcome for such a comprehensive study. With the availability of recently completed broadband network which consists of 3 digital broadband stations, and sufficient amount data of small magnitude shallow crustal events at near to medium-source distances, the authors were able to undertake a study to find coda Q value for the Sri Lankan Precambrian crust. Digital high-gain records of 13 small to micro earthquakes, magnitude varying from M_L 1.5 to 3.6 in local magnitude scale, has been processed for the analysis. The standard single scattering model, which demands the decay rates of backscattered coda waves that located at the tail part of seismograms, was used to estimate coda Q.

2. Q VALUE AND THE SINGLE BACKSCATTERING METHOD

Q value alias "the wave transmission quality factor" is merely regarded as a region specific property, which may highly depend on regional crustal characteristics such as age and composition of the crust, degree of heterogeneity, amount of asperities and irregularities, etc. There are several well established methods available in determining Q value for a region, out of which coda Q methods and spectral analysis methods are being popular in the current seismological practice. However, selection of a method to be applied in a region would evolve with the fundamental assumptions associated with the specific method. For example, single backscattering coda Q method proposed by Aki (1969), postulates coda waves as a derivative of surface waves which are singly scattered at acute angles in a heterogeneous medium, and the scattering is isotropic. Isotropic scattering means the medium considered itself is isotropic as well as the scattering taking place at a given heterogeneity is uniform in all directions despite the direction of the wave travel prior to the scattering. Furthermore, the method omits station-source distances during the calculation, given the epicentral paths are short enough to neglect. Hence, the method would best to use in a less complex medium which can be hypothesized as isotropic, at short site-source distances, otherwise due modifications need to be addressed. On the other hand, spectral analysis techniques in which empirical attenuation equations are fitted to observed Fourier spectral amplitudes, have shown to be widely adopted in regional studies that handle large amount of data at teleseismic distances. Although, the method is advantageous to determine the actual shape of Q which directly relates to the strong motion part (shear window) of a seismogram, one must be careful to apply the proper attenuation relationship which encompasses all possible means of attenuation for the subject region.

Aki and Chouet (1975) introduce following formulae to interpret the shape of coda amplitude decay with the lapse time;

$$P(\omega|t) = St^{-1}e^{-\omega t/Q} \qquad \text{(Surface waves)} \qquad (1)$$

$$P(\omega|t) = St^{-2}e^{-\omega t/Q} \qquad \text{(Body waves)} \qquad (2)$$

Here, $P(\omega|t)$ is the power spectral density of coda wave at time t. S is the source factor and ω is the circular frequency which is equal to $2\pi f$, where f is wave frequency. Q is the frequency dependent wave transmission quality factor. During the derivation, coda waves are assumed to be singly backscattered (scattered at acute angles) at discrete heterogeneities which are uniformly distributed in the isotropic medium. Energy loss in direct waves which are not subjected to scattering and any effect due to downward scattering (into the upper mantle) have been neglected. Furthermore, the above equations are theoretically valid in a collocated source-receiver condition, yet, modified relationships to account distance effect especially for long-distant events are also available in the literature (Kopnichev 1975, Pulli 1984, Sato 1977, Woodgold 1990). Energy contribution from the multiple scattering is considered minimal in effect, and hence ignored for the coda decay rate. Wu and Aki (1988) suggest Q value estimated in this way by coda decay rates would represent both attenuation effects, i.e., intrinsic attenuation and scattering effects, however effect of scattering over the decay rate would depend on amount of scattering taking place within the medium. When the scattering is weak the decay rate would depend on both (intrinsic and scattering), while when it is strong (as in a defuse medium) the rate depends only on intrinsic attenuation. Despite its difficulty in estimating individual contribution of each effect over the decay rate, efforts have been given sometimes to separate intrinsic Q from scattering Q (Hoshiba 1993, Zeng et al 1991). Further extensions of the method such as multiple scattering model (Gao et al 1983) takes effects due to multiply scattered phases into account in a heterogeneous medium.

Since the wave amplitude is proportional to square root of energy, writing above equations in terms of amplitude and taking natural logarithm would yield;

$$\ln[A(f,t).t^{0.5}] = \ln S' - \pi f t/Q \qquad \text{(Surface waves)} \qquad (3)$$

$$\ln[A(f,t).t] = \ln S' - \pi f t/Q \qquad \text{(Body waves)} \qquad (4)$$

Where, $A(f,t)$ denotes coda wave amplitude at time t for a given frequency f and S' represents the modified source term that corresponds to amplitude. In both equations (3) and (4), the logarithm of the product of wave amplitude and lapse time (the term in left side) exhibits a linear variation with lapse time (in 2nd term in right side) where the amplitude is multiplied by $t^{0.5}$ and by t, for surface and for body waves, respectively. Equations also indicate the geometric spreading rate for surface waves is about square root of that for body waves. Q value for a given frequency can be found by the slope of the linear fit defined in equation (3) or (4). The intercept of the linear fit which represents so-called "source term" can be sometimes merged with upper crustal attenuation term parameterized by Kappa (discussed in section 3), though the slope does not affect such an amalgamation, given Kappa remains constant with lapse time. Therefore, Q value estimated in this way by fitting envelopes in time domain can be considered as a reliable measure to represent the crustal quality in regional seismic wave transmission. Amplitude is calculated as the RMS (Root Mean Square) average of a moving time window, in which the window size can typically be of 3 s for short period waves (Havskov and Ottemoller 2010). Here, the RMS average appears to be suited well since its better representation of total energy absorbed within the window. The starting time of coda envelope in order to employ in the backscattering model, has been mostly taken as the time twice after S or Lg arrival (Singh and Herrmann 1983). Further studies reveal that about thrice after S or Lg, the coda arrival has permanently been established (Rautian and Khalturin 1978). Early coda available immediately after S or Lg, are often omitted in the decay rate calculation, mainly due to the fact which they are not being

susceptible for backscattering. On the contrary, late coda coming not less than twice after *S* or *Lg*, show a steady rate of decay which is free from undue instabilities such as sudden spikes and humps with respect to early coda, making the decay rate almost as independent of the travelled distance. A sample seismogram band pass filtered between 1-19 Hz, indicating essential phase arrivals and coda length to be used in a coda Q study, is shown in Figure 1. There has been a debate on which the coda waves are composed of, whether from surface waves or from body waves. In early studies many researches used to adopt coda as superimposed surface waves which are generated by incidence of primary waves at randomly distributed heterogeneities (Aki 1969, Herrmann 1980, Kopnichev 1975). However, soon later, body wave approximation has also been proposed to explain the behaviour of coda (Pulli 1984, Sato 1977). During the current study, again it was presumed the coda as singly backscattered body waves suggesting equation (4) to be valid in Q estimation. In addition to aforementioned Born assumptions which are bound with the single backscattering method, wave mode conversion at a heterogeneity such as a primary body wave to a secondary surface wave and vice versa, was assumed to be not incidental for the purpose of applying equation (4).
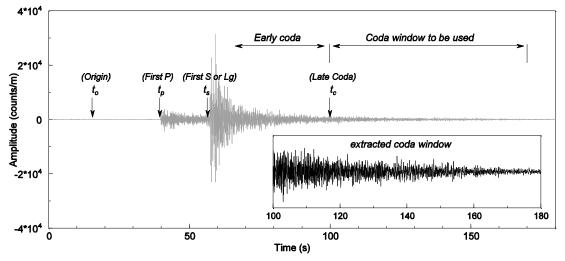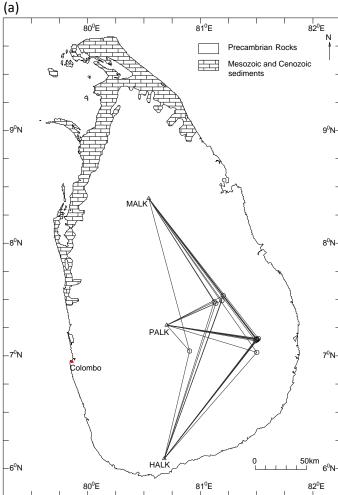

Figure 1. A sample seismogram band pass filtered between 1-19 Hz, indicating origin, essential phase arrivals and coda length to be used in a coda Q study. Extracted coda window to be used is shown as an insert. Event-M_L 3.5 at HALK, Hypocentral distance is 109 km.

Data base in the study consisted a total of 13 shallow crustal local events with magnitude ranging between M_L 1.5-3.6. While the hypocentral distance varied from 35 to 185 km, in terms of level of intensity the events would fall within the range of micro-tremor to small magnitude. Details of event data are given in Appendix, Table A1, whereas station-source paths to be used in the analysis and magnitude-hypocentral distance variation are shown in Figure 2. Location and origin time of events were determined based on "the flat earth layered velocity model", which has been considered to be reliable for estimations within local distances. Local magnitude was determined by the maximum amplitude picked in a filtered (between 1.25-19.75 Hz) standard Wood-Anderson seismogram. All processing steps including coda Q determination have been carried out using tools provided in SEISAN package (Havskov and Ottemöller 2012). The country's broadband seismic network comprises of digital stations located at Pallekelle (PALK), Hakmana (HALK) and Mahakanadarawa (MALK) rock sites. Seismograms recorded at high-gain channels having sample rates of 40 and 50 for PALK and for the latter two, respectively, were selected for the processing. Both horizontal and vertical components were used in the study in order to enlarge the size of the original sample. Variation of horizontal amplitude with respect to

vertical has shown to be insignificant in practical situations owing to negligible upper crustal amplification associated with the region's uppermost crust (Venkatesan and Gamage in Press), and this permitted both components to be considered as identical for the study. Main purpose was to increase the sample size and hence to avoid any error which can be arisen as being a smaller sample.
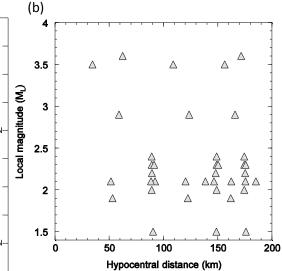
(a)

(b)

Figure 2. Earthquake data used in the study. (a) Station-source paths for the data set. Circles denote earthquakes while triangles represent broadband stations. Extent of the Precambrian crust is also indicated. (b) Distribution of the data set in magnitude and hypocentral distance space. Magnitude ranges from M_L 1.5 to 3.6, whereas hypocentral distance varies between 35 and 185 km.

Each seismogram was filtered by a 6-pole Butterworth filter applied at eight different pass-bands with centre frequencies 4, 6, 8,..., 18 Hz. Since low frequency amplitudes (less than about 2 Hz) sometimes caused low resolution quantisation problems due to poor signal strength, they have been omitted in calculation. Pass-bands were defined to comply with a constant relative bandwidth of 0.5, which resulted bandwidths to be in the form 4±1, 6±1.5, 8±2,…, 18±4.5 for selected centre frequencies. $A(f, t)$ for a given centre frequency was then calculated by the RMS average of a moving 5-cycle (5f) window as described in Havskov et al (1989). In the present study, coda length starting time was hardwired to 2 times S or Lg arrival time because of its optimal use in the backscattering model in both viewpoints of having a steady decay rate which is uncontaminated with early coda (discussed previously), and of following the consistency in the method for the purpose of comparison results with other regions. A slightly lower average Vp/Vs ratio of about 1.73 was resulted for the data in arrival time calculation, and was retained same for selecting the coda length. A fixed coda length was applied at a turn for the data set, and the entire process was repeated for four different coda window cases as 40, 50, 60 and 70 s. Finally, an average Q representing all windows has been estimated. A parametric study extending beyond a single time window case has been undertaken to investigate the time dependent behaviour of Q, if any. A number

of studies evidence on increase of coda Q with the time (Gusev 1995, Kvamme and Havskov 1989, Pulli 1984), seemingly, due to magnifying multiple scattering effects as sampling larger volumes at higher crustal depths. Moreover, the effective earthquake duration which depends mainly on magnitude-distance parameters, can partly affect the final uniformity in coda windows. Therefore, a parametric study has been implemented to explore the variation of Q over time and thus to derive a value which would represent the average behaviour. 40 s as the lower limit was considered adequate to have stable results, whereas the upper limit, 70 s, was chosen as a compromise of retaining sufficient data which have higher signal strength for the final processing. Signal to Noise (S/N) ratio was calculated by the ratio between RMS amplitude of the last 5 s of the filtered coda window and that of the noise window preceding first P arrival. Q values resulted with S/N ratio below 3 were eliminated from final results. Consequently, linear fits to coda envelopes given in equation (4), which were unable to indicate a 50% of minimum correlation, have also been omitted. Two sample plots indicating coda amplitude decay with respect to the lapse time for two randomly selected centre frequencies (4 and 14 Hz) are shown in Figure 3. It can be seen that the coda amplitude diminishes approximately linearly (in the log scale) with the time due to above discussed attenuation and scattering effects, and the apparent rate of decay which denoted by the slope, is higher at 14 Hz than at 4 Hz indicating the decay is rapid in high frequency waves.
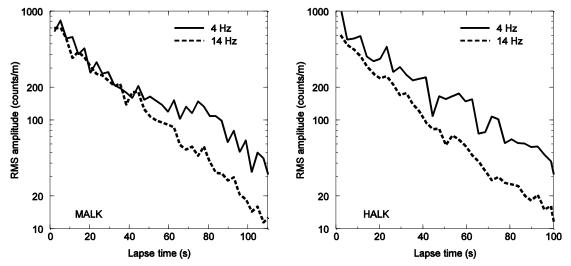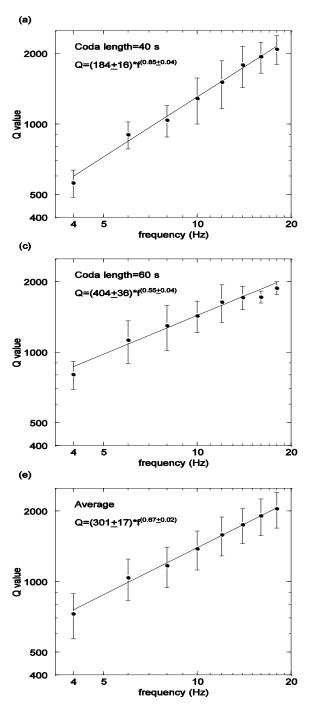

Figure 3. Decay of coda amplitude (RMS value) with the lapse time at two random centre frequencies (4 and 14 Hz). The apparent rate of decay denoted by the slope is higher at 14 Hz than at 4 Hz, indicating a rapid decay in high frequency waves. Laps time "0" is relevant to start of the coda window. Two plots are for the event M_L 3.5.

3. RESULTS AND DISCUSSION

Resulted Q values at selected centre frequencies in each time window are shown in Table 1 and in Figure 4. Q at 1 Hz termed as Q_0 and n (exponent) resulting from weighted linear regression of $Q = Q_0 f^n$ (Mitchell 1981) are given in each case. Comparably higher Q_0 values were resulted except at 40 s time window case, in which a lower value of $Q_0 = 184 \pm 16$ would be attributed to sampling a smaller volume which encircles mainly a younger upper portion of the crust. Besides, multiple scattering effects (although nullified in the single backscattering method), which may cause magnification of "scattering Q", would induce observed increments in Q_0 with the time. The increasing trend is shown to be clear up to 60 s window case, and then after at 70 s Q_0 has again dropped to 368±35. Since, the variation of Q_0 over the length of time window was rather noticeable, an average value for all time window cases was considered to better represent the overall behaviour in Q_0 of the region.

Therefore, average Q values of all four cases were found and the respective weighted linear fit was setup to estimate average Q_0 and n values which were resulted as 301 ± 17 and 0.67 ± 0.02, respectively (Figure 4e).
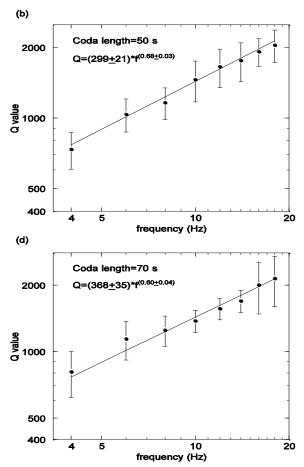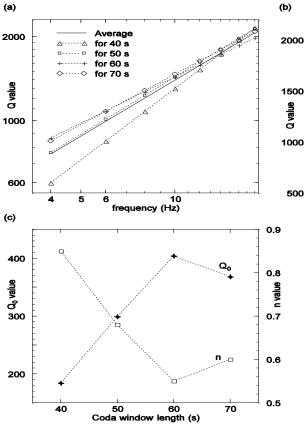

Figure 4. Resulted Q values with standard deviations at selected centre frequencies are shown in each coda window length case. Solid lines represent weighted linear least squares fits of $Q = Q_0 f^n$. (a) For 40 s. (b) For 50 s. (c) For 60 s. (d) For 70 s. (e) Average Q values and the respective weighted linear fit for all cases.

Frequency (Hz)	Q values for selected coda time windows (N is number of obs.)								Ave. for all cases	N
	40 s	N	50 s	N	60 s	N	70 s	N		
4 (3-5)	561±75	7	735±132	10	804±111	12	810±191	9	729±160	38
6 (4.5-7.5)	901±119	18	1037±167	21	1127±232	18	1142±227	16	1040±209	73
8 (6-10)	1039±159	20	1163±181	17	1298±284	18	1251±197	14	1171±230	69
10 (7.5-12.5)	1286±286	20	1459±288	19	1430±220	14	1379±160	11	1381±260	64
12 (9-15)	1510±349	19	1656±310	16	1638±300	13	1566±175	11	1586±301	59
14 (10.5-17.5)	1787±358	20	1759±332	15	1713±197	10	1697±195	9	1750±298	54
16 (12-20)	1941±294	11	1920±260	10	1720±102	6	2007±526	9	1910±340	36
18 (13.5-22.5)	2087±292	10	2046±325	8	1879±120	6	2147±550	8	2049±357	32

Q_0 (Q at 1 Hz)	184±16	299±21	404±36	368±35	301±17
n (exponent)	0.85±0.04	0.68±0.03	0.55±0.04	0.6±0.04	0.67±0.02

Table 1. Resulted Q values from the single backscattering method

Variation of Q with respect to the coda time window has shown in Figure 5. Figure 5b clearly illustrates individual variation of average Q with the length of coda window used in each case, where it evidences an increasing trend of average Q with the time at low frequencies and a reverse trend at high frequencies. The increase of low frequency Q is more pronounced at frequencies below say 8 Hz, while the high frequency Q reduction is apparent at frequencies above 14 Hz. The probable reason behind Q increase with the length of time window would be related to earlier discussed time dependency in scattering Q which is mainly governed by the facts; sampling deeper volumes in much denser crust and enhancing multiple scattering effects. Both these would reduce the rate of coda amplitude decay resulting higher Q values with the time. Moreover, it shows the rate of Q increase over the time window is substantial between 40-60 s window range, and then after at 70 s the rate seems trivial as more like saturated. In contrary, Q reduction at high frequencies is hard to ascertain and appears to be a minor trend due to its limited consistency shown for the whole range of coda lengths. However, this can be resulted partially as an artifact of reducing number of observations when increasing the coda length from 40 to 60 s (see Table 1), which may have caused elimination of observations with higher Q values. Reduction in Q with the time for a given frequency is less likely to happen as a result of increasing the decay rate, unless any localized trend is there in the seismogram. On the other hand, discernible trade-offs which can sometimes alter final results, may arise due to many possible reasons; being a smaller data sample recorded at a smaller network, being an inhomogeneous medium with various unrevealed irregularities in the crust, inconsistency due to the combined effect of single and multiple scattering, and any other uncertainty due to not being compatible with basic assumptions of the method set at the outset.
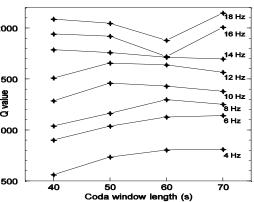

Figure 5. Variation of Q with the length of coda window. (a) Comparison of $Q = Q_0 f^n$, with respect to the length of coda window. (b) Individual Q comparison with the length of coda window. (c) Q at 1 Hz (Q_0) and "exponent", n, variation with the coda window length. A rapid variation in both coefficients is apparent between 40 to 60 s window cases.

Resulted average Q_0 value 301±17 would have a consistency with the country's basement rocks underlain. A comparably higher Q_0 yields a lesser anelastic attenuation during seismic wave travel through the medium which comprises with harder/older rocks. Many sources indicate more than 90% of Sri Lanka's crustal rocks consists with Crystalline rocks of Precambrian whose age can be as old as about 2000 Ma (Cooray 1994, Kroner and Brown 2005). Geochronological studies have further confirmed the sedimentation process of the crust in central part of the country has been completed during Palaeoproterozoic era (Barber 2000, Mathavan et al 1999), which belongs to the late Precambrian period. By referring to the country's geology, one may argue that the inferred Q_0 does not seem to reflect its complete characteristics of a crust of typical Precambrian, since relatively much higher Q_0 values than this are quite common to observe in such regions; Canadian shield-893 (Atkinson 2004), Indian shield-800 (Singh et al 2004), Western Australia-457 (Allen et al 2006). However, the authors believe Q_0 calculation can be influenced by local characteristics of the uppermost rocks as well. The effect can be crucial in situations where a thin lining of younger Sedimentary stratum rests on top of the older Precambrian crust. A similar scenario can also be susceptible for the Sri Lankan crust. A rapid increase of Q_0 with the coda window length starting from 184±16 at 40 s window to 404±36 at 60 s, would attest the difference of characteristics in vertical crustal profile in terms of the volume sampled, which the scattering has taken place, from a younger upper crust to a much older deeper crust underlain (sometimes may extend to the upper mantle), respectively. Therefore, the estimated Q_0 which parameterizes attenuations along the whole travel path can immensely depend on nature of the uppermost part, although attenuation effects in the upper crust alone are separately parameterized. Malagnini et al (Malagnini et al 2002, Malagnini et al 2000) based on spectral analysis have also determined relatively higher Q_0 values as 400 (n=0.42) and 260 (n=0.55), with at the same time moderate Kappa values of 0.05 and 0.045, for central Europe and for Northeastern Italy, respectively. Other comparable estimations of Q_0 may include Northwestern United States, Q_0=300, n=0.3 (Singh and Herrmann 1983); Guangdong-China, Q_0=370, n=0.4 (Jin and Aki 1988). Venkatesan and Gamage (Venkatesan and Gamage in Press) have determined a similar regional Q_0 value of about 389 for northern Indian Oceanic crust surrounding Sri Lanka based on a spectral analysis of moderate shallow events that occurred at long distances. However, this regional Q_0, which is mostly characterized by the properties of northern Indian Oceanic crust that has abundance of thinner diffused formations, would not probe a direct comparison with the local coda Q_0 estimated in the current study, mainly because of the difference in two crustal structures. Many studies have shown the regional seismic wavefield in an oceanic crust can be significantly different from that in a continental crust (Campillo 1990, Kennett 1985, Knopoff et al 1979). Hence, the wave traverse pattern and the final content of waves which are guided through a thinner oceanic crust such as northern Indian Ocean, can be considerably different from that in a typical thicker continental crust such as the one underlying Sri Lanka.

4. CONCLUSION

Attenuation characteristics in Sri Lankan Precambrian crust have been investigated analysing digital waveform data of small and micro earthquakes that recorded at the country's broadband network. Application of the single backscattering coda wave method with varying coda window length revealed a considerable time dependency in estimated Q, supporting previous observations in coda Q studies. An increase of Q with the coda length especially at low frequencies ($\leq$ 8 Hz) and a minor reverse trend at high frequencies ($\geq$ 14 Hz), can be noted in the selected frequency range, which in turn resulted higher Q_0 values at longer time windows. Increasing scattering Q due to multiple scattering effects and sampling much larger volumes at deeper crust can result higher Q with the time. The average coda Q for all time

window cases has followed the form, $Q = (301 \pm 17)f^{(0.67 \pm 0.02)}$. This would agree with the type of crust underneath the country which is of Precambrian, yet a thinner sedimentary layer on above is susceptible.

ACKNOWLEDGEMENT

REFERENCES

Aki, K. (1969). Analysis of the seismic coda of local earthquakes as scattered waves, J Geophys Res **74** 615-631.

Aki, K., and B. Chouet (1975). Origin of coda waves: Source, attenuation, and scattering effects, J Geophys Res **80** 3322-3342.

Allen, T. I., T. Dhu, P. R. Cummins, and J. F. Schneider (2006). Empirical Attenuation of Ground-Motion Spectral Amplitudes in Southwestern Western Australia, Bull Seismol Soc Am **96** 572-585.

Atkinson, G. M. (2004). Empirical Attenuation of Ground-Motion Spectral Amplitudes in Southeastern Canada and the Northeastern United States, Bull Seismol Soc Am **94** 2419-2423.

Atkinson, G. M. (2005). Ground Motions for Earthquakes in Southwestern British Columbia and Northwestern Washington: Crustal, In-Slab, and Offshore Events, Bull Seismol Soc Am **95** 1027-1044.

Atkinson, G. M., and D. M. Boore (1995). Ground-motion relations for eastern North America, Bull Seismol Soc Am **85** 17-30.

Barber, A. J. (2000). Geological Map of Central and Western Sri Lanka: Provisional Series 1997 — scale 1:250,000, and seven 1:100,000 map sheets. Geological Survey and Mines Bureau, Sri Lanka, and the British Geological Survey. US$10.00+postage, J Asian Earth Sci **18** 509-512.

Campillo, M. (1990). Propagation and attenuation characteristics of the crustal phaseLg, Pure Appl Geophys **132** 1-19.

Cooray, P. G. (1994). The Precambrian of Sri Lanka: a historical review, Precambrian Res **66** 3-20.

Gamage, P., and S. Venkatesan (2012). Seismic risk analysis based on historical events reported in Sri Lanka, in *22nd Australasian Conference on the Mechanics of Structures and Materials, ACMSM22* B. Samali, M. M. Attard and C. Song (Editors), Sydney, Australia, 437-442.

Gao, L. S., L. C. Lee, N. N. Biswas, and K. Aki (1983). Comparison of the effects between single and multiple scattering on coda waves for local earthquakes, Bull Seismol Soc Am **73** 377-389.

Gusev, A. A. (1995). Vertical profile of turbidity and coda Q, Geophys J Int **123** 665-672.

Havskov, J., S. Malone, D. McClurg, and R. Crosson (1989). Coda Q for the state of Washington, Bull Seismol Soc Am **79** 1024-1038.

Havskov, J., and L. Ottemo¨ller (2012). SEISAN: The Earthquake Analysis Software for Windows, Solaris and Linux, Version 8.0 U. o. B. Institute of Solid Earth Physics, Norway. (Editor).

Havskov, J., and L. Ottemoller (2010). Routine Data Processing in Earthquake Seismology With Sample Data, Exercises and Software, Springer.

Herrmann, R. B. (1980). Q estimates using the coda of local earthquake, Bull Seismol Soc Am **70** 447-468.

Hoshiba, M. (1993). Separation of scattering attenuation and intrinsic absorption in Japan using the multiple lapse time window analysis of full seismogram envelope, J Geophys Res: Solid Earth **98** 15809-15824.

Jin, A., and K. Aki (1988). Spatial and temporal correlation between coda Q and seismicity in China, Bull Seismol Soc Am **78** 741-769.

Kennett, B. L. N. (1985). On regional S, Bull Seismol Soc Am **75** 1077-1086.

Knopoff, L., R. G. Mitchel, E. G. Kausel, and F. Schwab (1979). A search for the oceanic Lg phase, Geophys J Int **56** 211-218.

Kopnichev, Y. F. (1975). A model of generation of the tail of the seismogram, Doklady Earth Science Sections **222** 13-15.

Kroner, A., and L. Brown (2005). Structure, Composition and Evolution of the South Indian and Sri Lankan Granulite Terrains from Deep Seismic Profiling and Other eophysical and Geological Investigations: A LEGENDS Initiative, Gondwana Research **8** 317-335.

Kvamme, L. B., and J. Havskov (1989). Q in southern Norway, Bull Seismol Soc Am **79** 1575-1588.

Lam, N., J. Wilson, and G. Hutchinson (2000). Generation of synthetic earthquake accelerograms using seismological modelling: A review, J Earthquake Eng **4** 321-354.

Malagnini, L., A. Akinci, R. B. Herrmann, N. A. Pino, and L. Scognamiglio (2002). Characteristics of the Ground Motion in Northeastern Italy, Bull Seismol Soc Am **92** 2186–2204.

Malagnini, L., R. B. Herrmann, and K. Koch (2000). Regional Ground-Motion Scaling in Central Europe, Bull Seismol Soc Am **90** 1052-1061.

Mathavan, V., W. K. B. N. Prame, and P. G. Cooray (1999). Geology of the High Grade Proterozoic Terrains of Sri Lanka, and the Assembly of Gondwana: an Update on Recent Developments, Gondwana Research **2** 237-250.

Mitchell, B. J. (1981). Regional variation and frequency dependence of Qβ in the crust of the United States, Bull Seismol Soc Am **71** 1531-1538.

Pulli, J. J. (1984). Attenuation of coda waves in New England, Bull Seismol Soc Am **74** 1149-1166.

Rautian, T. G., and V. I. Khalturin (1978). The use of the coda for determination of the earthquake source spectrum, Bull Seismol Soc Am **68** 923-948.

Royer, J. Y., and R. G. Gordon (1997). The motion and boundary between the Capricorn and Australian plates, SCIENCE **277** 1268-1274.

Sato, H. (1977). Energy propagation including scattering effects: Single isotropic scattering approximation, Phys Earth Planet In **25** 27-41.

Singh, S., and R. B. Herrmann (1983). Regionalization of crustal coda Q in the continental United States, J Geophys Res: Solid Earth **88** 527-538.

Singh, S. K., D. García, J. F. Pacheco, R. Valenzuela, B. K. Bansal, and R. S. Dattatrayam (2004). Q of the Indian Shield, Bull Seismol Soc Am **94** 1564-1570.

Stein, S., and E. A. Okal (1978). Seismicity and tectonics of the Ninetyeast Ridge area: Evidence for internal deformation of the Indian plate, J. Geophys. Res. **83** 2233-2245.

Venkatesan, S., and P. Gamage (in Press). Spectral analysis of seismic waves in the northern Indian Ocean region, Bull Seismol Soc Am.

Wiens, D. A., S. Stein, C. DeMets, R. G. Gordon, and C. Stein (1986). Plate tectonic models for Indian Ocean. "intraplate" deformation, Tectonophysics **132** 37-48.

Wimalaratne, K. D. (1993). The First Earthquake Recorded in Sri Lanka, in *Daily News*.

Woodgold, C. R. D. (1990). Estimation of Q in eastern Canada using coda waves, Bull Seismol Soc Am **80** 411-429.

Wu, R.-S., and K. Aki (1988). Multiple scattering and energy transfer of seismic waves—Separation of scattering effect from intrinsic attenuation II. Application of the theory to Hindu Kush region, Pure Appl Geophys **128** 49-80.

Zeng, Y., F. Su, and K. Aki (1991). Scattering wave energy propagation in a random isotropic scattering medium: 1. Theory, J Geophys Res: Solid Earth **96** 607-619.

APPENDIX

Table A1. List of events used in the study.

Date	Time (UTC)	Lat.	Long.	Depth (km)	Local magnitude (M_L)
19/05/2012	20:14:36	7.04	80.91	7	3.5
26/05/2012	16:22:06	7.54	81.20	15	3.6
18/06/2012	16:37:54	7.48	81.12	4	2.1
28/08/2012	10:12:47	7.49	81.19	10	2.9
31/08/2012	14:34:46	7.13	81.49	10	2.1
14/09/2012	23:41:19	7.47	81.14	10	1.9
28/09/2012	23:56:11	7.03	81.50	10	2.1
1/12/2012	2:47:46	7.15	81.50	10	2.3
1/12/2012	3:31:32	7.15	81.52	10	2.3
1/12/2012	11:09:33	7.14	81.50	10	2.2
14/12/2012	7:35:05	7.14	81.51	10	1.5
25/01/2013	4:04:30	7.15	81.50	10	2.0
25/01/2013	5:08:22	7.15	81.50	10	2.4